



OXFORD

OXFORD TEXTBOOKS IN CRITICAL CARE

Oxford Textbook of Advanced Critical Care Echocardiography

EDITED BY

Anthony McLean

Stephen Huang

Andrew Hilton

ALL CONTENT AVAILABLE AT OXFORDMEDICINE.COM

Oxford Textbook of

**Advanced
Critical Care
Echocardiography**

Oxford Textbook of

Advanced Critical Care Echocardiography

EDITED BY

Anthony McLean

*Professor and Director, Intensive Care Medicine, Sydney Medical School and Nepean Hospital,
University of Sydney, New South Wales, Australia*

Stephen Huang

*Professor, Intensive Care Medicine, Sydney Medical School and Nepean Hospital,
University of Sydney, New South Wales, Australia*

Andrew Hilton

*Clinical Associate Professor and Deputy Director of ICU
Intensive Care Unit, Austin Hospital and Melbourne University, Victoria, Australia*

OXFORD
UNIVERSITY PRESS

OXFORD

UNIVERSITY PRESS

Great Clarendon Street, Oxford, OX2 6DP,
United Kingdom

Oxford University Press is a department of the University of Oxford.
It furthers the University's objective of excellence in research, scholarship,
and education by publishing worldwide. Oxford is a registered trade mark of
Oxford University Press in the UK and in certain other countries

© Oxford University Press 2020

The moral rights of the authors have been asserted

First Edition published in 2020

Impression: 1

All rights reserved. No part of this publication may be reproduced, stored in
a retrieval system, or transmitted, in any form or by any means, without the
prior permission in writing of Oxford University Press, or as expressly permitted
by law, by licence or under terms agreed with the appropriate reprographics
rights organization. Enquiries concerning reproduction outside the scope of the
above should be sent to the Rights Department, Oxford University Press, at the
address above

You must not circulate this work in any other form
and you must impose this same condition on any acquirer

Published in the United States of America by Oxford University Press
198 Madison Avenue, New York, NY 10016, United States of America

British Library Cataloguing in Publication Data

Data available

Library of Congress Control Number: 2019950166

ISBN 978-0-19-874928-8

Printed in Great Britain by
Bell & Bain Ltd., Glasgow

Oxford University Press makes no representation, express or implied, that the
drug dosages in this book are correct. Readers must therefore always check
the product information and clinical procedures with the most up-to-date
published product information and data sheets provided by the manufacturers
and the most recent codes of conduct and safety regulations. The authors and
the publishers do not accept responsibility or legal liability for any errors in the
text or for the misuse or misapplication of material in this work. Except where
otherwise stated, drug dosages and recommendations are for the non-pregnant
adult who is not breast-feeding

Links to third party websites are provided by Oxford in good faith and
for information only. Oxford disclaims any responsibility for the materials
contained in any third party website referenced in this work.

*We dedicate this book to our good friend and colleague Donald Stewart (1950–2015).
His resourceful and clever contributions over many years greatly enhanced
our understanding and development of critical care ultrasound.
His premature and tragic death took away a true pioneer in the field.*

Preface

Echocardiography has become an integral and essential part of daily practice in the critical care setting. The rapid and immediate application of this invaluable tool must be matched by an appropriate set of operator skills and knowledge. The critical care physician, pivotal to this enhancement in patient management, must learn a broad range of techniques and knowledge when moving beyond the basic level of echocardiography to the more advanced level. This book is dedicated to assisting critical care physician in this challenging and rewarding pursuit.

To provide guidance in how to optimize the use of echocardiography in the evaluation of cardiac function and haemodynamics in the critically ill patient, contributions from international experts have been brought together in this book. The book is divided into four parts. Part I (General Principles) provides the building blocks for advanced critical care echocardiography. Doppler principles, artefacts, and pitfalls, haemodynamic, and cardiopulmonary principles are covered. Part II (Echo Assessments) contains 12 chapters; each describes the techniques and assessment methods used in specific clinical topics. Part III (Integrative Approach) marks the full applications of critical care

echocardiography in different but common scenarios. The contents range from those commonly encountered situations to the unexpected and unusual. Echocardiography is a very live technology and has been evolving in the last 30 years. Covering only the conventional techniques without describing the latest would be a major omission in an advanced echocardiography book. Part IV (Future Developments) therefore covers the latest techniques that are available at present.

We are indebted to all colleagues in the field who have been working humbly and silently in the background giving life to critical care echocardiography, and to those who contributed to this book in many ways. We have attempted to be as accurate and up to date as possible, but we recognize that any work of this scale may contain mistakes, omissions, and outdated information. We will be grateful if you can bring such items to our attention.

We hope that this book provides a valuable resource to teachers, students, researchers, and practitioners of critical care echocardiography. Clinicians undertaking this journey into more advanced echocardiographic techniques will find it an enthralling and lifelong endeavour.

Contents

Abbreviations xi
Contributors xiii
Digital media accompanying the book xv

PART I

General Principles

1. **Basic Doppler principles** 3
Stephen Huang
2. **Common Doppler artefacts and pitfalls** 21
Stephen Huang
3. **Haemodynamics for echocardiography** 37
Stephen Huang
4. **Cardiac mechanics** 53
Stephen Huang
5. **Heart–lung interactions** 73
Gulrukh Zaidi and Paul H. Mayo

PART II

Echo Assessments

6. **Left ventricular systolic function** 83
Nick Fletcher
7. **Left ventricular diastolic function** 93
Andrew Hilton
8. **Right ventricular function** 119
Michelle S. Chew
9. **Pulmonary hypertension** 133
Michel Slama and Julien Maizel
10. **Preload and fluid responsiveness** 141
Philippe Vignon
11. **Cardiac output measurement** 153
Stephen Huang

12. **Pericardial effusion and cardiac tamponade** 165
Andrew Hilton
13. **Dynamic left ventricular outflow tract obstruction** 191
Daniel de Backer
14. **Valvular stenosis** 195
Ana Martinez-Naharro and Susanna Price
15. **Valvular regurgitation** 207
Gordon YS Choi and Yu-Yeung Yip
16. **Adult congenital heart disease** 225
Andrew Hilton
17. **Miscellaneous: Thoracic aortic disease, complications of acute myocardial infarction, and constrictive pericarditis** 255
Anthony McLean

Part III

Integrative Approach

18. **Hypotension** 265
Frances Colreavy
19. **Acute pulmonary embolism** 275
Anthony McLean
20. **Septic shock** 281
Michelle S. Chew
21. **Acute respiratory failure** 287
Martin Balik
22. **Echocardiography in a patient with chest pain—an integrated approach** 295
Anthony McLean
23. **Echocardiography in postcardiac surgery** 301
Susanna Price

24. **Echocardiography in trauma** 311
Vindodh Nanjayya
25. **Haemodynamic assessments in mechanically ventilated patients: A focus on blood pressure respiratory variations** 321
Antoine Vieillard-Baron
-
- Part IV**
Future Developments
26. **Strain, twist, and torsion in left ventricular assessment** 329
Stephen Huang
27. **Strain imaging in right ventricle assessment** 343
Sam Orde
28. **Contrast echocardiography** 351
Sam Orde
29. **3D echocardiography in intensive care** 359
Konstantin Yastrebov
30. **Accreditation in advanced critical care echocardiography** 365
Anthony McLean
- Index* 369

Abbreviations

AF	atrial fibrillation	IR	isovolumic relaxation
AHA	American Heart Association	ISHLT	International Society of Heart and Lung Transplantation
AL	anterior leaflet	IVC	inferior vena cava
AML	anterior mitral leaflet	IVS	interventricular septum
AP	anterior-posterior	KE	kinetic energy
AR	aortic regurgitation	LA	left atrium
ARDS	acute respiratory distress syndrome	LAA	left atrial appendage
ARV	atrialized right ventricle	LAP	left atrial pressure
AS	aortic stenosis	LBBB	left bundle branch block
ASD	atrial septal defect	LV	left ventricle
ASE	American Society of Echocardiography	LVEDP	left ventricular end-diastolic pressure
AUC	area under the curve	LVEDV	left ventricular end-diastolic volume
AVA	aortic valve area	LVEF	left ventricular ejection fraction
AVO	aortic valve opening	LVH	left ventricular hypertrophy
BAI	blunt aortic injury	LVOT	left ventricular outflow tract
BART	Blue Away, Red Towards	LVOTO	left ventricular outflow tract obstruction
BP	blood pressure	LVP	left ventricular pressure
BSA	body surface area	MAPSE	mitral annular plane systolic excursion
CCE	critical care echocardiography	MBE	modified Bernoulli equation
CFD	colour-flow Doppler	MI	myocardial infarction
CO	cardiac output	MODS	method of disc summation
COPD	chronic obstructive pulmonary disease	MPA	main pulmonary artery
CSA	cross-sectional area	MPAP	mean pulmonary arterial pressure
CT	computed tomography	MPI	myocardial performance index
CVP	central venous pressure	MR	mitral regurgitation
CW	continuous wave	MS	mitral stenosis
DPAP	diastolic pulmonary arterial pressure	MV	mitral valve
DSE	dobutamine stress echocardiography	MVA	mitral valve area
DT	deceleration time	MVC	mitral valve closure
ECMO	extracorporeal membrane oxygenation	PA	pulmonary artery
EF	ejection fraction	PACT	pulmonary artery acceleration time
ERS	European Respiratory Society	PAH	pulmonary arterial hypertension
ESC	European Society of Cardiology	PAP	pulmonary arterial pressure
FAC	fractional area change	PASP	pulmonary artery systolic pressure
FFT	fast Fourier transformation	PD	pulse duration
FL	false lumen	PE	pressure energy
FRC	functional residual capacity	PE	pulmonary embolism
FRV	functional right ventricle	PEEP	positive end-expiratory pressure
HFpEF	heart failure with preserved ejection fraction	PESI	Pulmonary Embolism Severity Index
HFrEF	heart failure with reduced ejection fraction	PFO	patent foramen ovale
HR	heart rate	PG	pressure gradient
IABP	intra-aortic balloon pump	PH	pulmonary hypertension
IC	isovolumic contraction	PHT	pressure half-time
ICU	intensive care unit	PISA	proximal isovelocity surface area
IPP	intrapericardial pressure	PLAX	parasternal long axis
IPPV	intermittent positive pressure ventilation		

PMC	percutaneous mitral commissurotomy	SEC	spontaneous echo contrast
PPAH	primary pulmonary arterial hypertension	SL	septal leaflet
PR	pulmonary regurgitation	SPAP	systolic pulmonary arterial pressure
PRF	pulse repetition frequency	STEMI	ST-elevation myocardial infarct
PRP	pulse repetition period	SV	stroke volume
PRV	pericardial effusion right ventricular	SVC	superior vena cava
PSAX	parasternal short axis	SW	spectral width
PSM	paradoxical septal motion	TAPSE	tricuspid annular plane systolic excursion
PVF	pulmonary venous flow	TAVI	transcatheter aortic valve implantation
PVR	pulmonary vascular resistances	TDI TA	tissue Doppler imaging of tricuspid annulus
PW	pulsed wave	TDI	tissue Doppler imaging
PWP	pulmonary wedge pressure	TL	true lumen
PWTD	pulsed-wave tissue Doppler	TOE	transoesophageal echocardiography
RA	right atrium	TOF	Tetralogy of Fallot
RAP	right atrial pressure	TR	tricuspid regurgitation
RBC	red blood cells	TS	tricuspid stenosis
RCA	right coronary artery	TTE	transthoracic echocardiogram
RCC	right coronary cusp	TV	tricuspid valve
RV	right ventricle	VARC	Valve Academic Research Consortium
RVESP	right ventricular end-systolic pressure	VHD	valvular heart disease
RVOT	right ventricular outflow tract	VR	velocity ratio
RVSV	right ventricular stroke volume	VSD	ventricular septal defects
SAM	systolic anterior motion	VTI	velocity time integral
SC	subcostal		

Contributors

Martin Balik Associate Professor, Department of Anaesthesiology and Intensive Care, First Faculty of Medicine, Charles University and General University Hospital, Prague, Czech Republic

Michelle S. Chew Professor, Senior Consultant, Department of Anesthesiology and Intensive Care, Linköping University Hospital, Sweden

Gordon Choi Consultant, Department of Anaesthesia and Intensive Care, Prince of Wales Hospital, The Chinese University of Hong Kong, Hong Kong

Frances Colreavy Associate Professor, University College Dublin School of Medicine; Consultant Intensivist, Mater Misericordiae Hospital, Dublin, Ireland

Daniel de Backer Professor, Department of Intensive Care, CHIREC Hospitals, Université Libre de Bruxelles, Brussels, Belgium

Nick Fletcher Consultant in Cardiac Critical Care and Cardiac Anaesthesia, Honorary Senior Lecturer, St Georges University Hospital, London, UK

Andrew Hilton Clinical Associate Professor and Deputy Director of ICU, Intensive Care Unit, Austin Hospital and Melbourne University, VIC, Australia

Stephen Huang Professor, Intensive Care Medicine, Sydney Medical School and Nepean Hospital, University of Sydney, Sydney, NSW, Australia

Julien Maizel Full Professor, Unité de réanimation médicale CHU Sud Amiens, France and unité INSERM 1066 université Picardie Jules Verne, Amiens, France

Ana Martinez-Naharro Peri-procedural Echocardiography Fellow, Royal Brompton Hospital, Sydney Street, London, UK

Paul H. Mayo Academic Director Critical Care, Division Pulmonary, Critical Care and Sleep Medicine, NSUH/LIJMC Northwell Health System; Professor of Clinical Medicine, Zucker School of Medicine at Hofstra/Northwell, NY, USA

Anthony McLean Professor and Director, Intensive Care Medicine, Sydney Medical School and Nepean Hospital, University of Sydney, Sydney, NSW, Australia

Vinodh Bhagyalakshmi Nanjaya Consultant ICU and Head, Cardiothoracic ICU, Critical Care Echocardiography and Ultrasound, The Alfred, Melbourne, VIC, Australia

Sam Orde Intensivist, Intensive Care Unit, Nepean Hospital, Sydney, NSW, Australia

Susanna Price Consultant Cardiologist and Intensivist and Honorary Senior Lecturer, Royal Brompton and Harefield NHS Foundation Trust and NHLI, Royal Brompton Hospital, London, UK

Michel Slama Full Professor and Chair of Critical Care, Unité de réanimation médicale CHU Sud Amiens, France and unité INSERM 1066 université Picardie Jules Verne, Amiens, France

Antoine Vieillard-Baron Professor and Department Head, Intensive Care Unit, University Hospital Ambroise Paré, Boulogne-Billancourt, France

Philippe Vignon Professor and Head Medical-surgical ICU, Medical-surgical ICU, Dupuytren Teaching Hospital, Limoges Cedex, France

Konstantin Yastrebov Associate Professor, University of New South Wales, Senior Specialist in Intensive Care and Head of Critical Care Echocardiography Program, St George Hospital, Sydney, NSW, Australia




Sunny Y.Y. Yip Associate Consultant, Department of Anaesthesia and Intensive Care, Prince of Wales Hospital, The Chinese University of Hong Kong, Hong Kong

Gulrukh Zaidi Attending Physician, Division Pulmonary, Critical Care and Sleep Medicine, NSUH/LIJMC Northwell Health System; Assistant Professor of Medicine, Zucker School of Medicine at Hofstra/Northwell, NY, USA

Digital media accompanying the book

Individual purchasers of this book are entitled to free personal access to accompanying digital media in the online edition. Please refer to the access token card for instructions on token redemption and access.

These online ancillary materials, where available, are noted with iconography throughout the book.

-  Videos
-  Cases
-  Multiple-choice questions

The corresponding media can be found on *Oxford Medicine Online* at: <https://www.oxfordmedicine.com/otadvancedecho>

If you are interested in access to the complete online edition, please consult with your librarian.

PART I

General Principles

1. **Basic Doppler principles** 3
Stephen Huang
2. **Common Doppler artefacts and pitfalls** 21
Stephen Huang
3. **Haemodynamics for echocardiography** 37
Stephen Huang
4. **Cardiac mechanics** 53
Stephen Huang
5. **Heart-lung interactions** 73
Gulrukh Zaidi and Paul H. Mayo

Basic Doppler principles

Stephen Huang

Introduction

The *International Expert Round Table on Ultrasound in ICU* report recommends two levels of critical care echocardiography credentials: Level 1 (basic) and Level 2 (advanced). Level 1 critical care echocardiography training only requires trainees to be competent in two-dimensional (2D) echocardiography measurements and interpretations (see Chapter 29) whereas Level 2 credential requires, among other things, haemodynamic assessments by Doppler echocardiography [1].

The usefulness of Doppler echocardiography can be appreciated from examining the *Doppler spectrum* in [Figure 1.1](#), which illustrates typical mitral inflow and regurgitation blood *velocity vs. time* relationship. It can be seen that the two Doppler spectra differ in the following aspects:

- shape
- velocity
- direction: positive vs. negative
- timing and duration

Physiologically, the differences observed in the aforementioned parameters can be explained by the instantaneous changes in pressure gradient between the two chambers, in this case the left ventricle and the left atrium. The pressure gradient between the two chambers can in turn be accounted for by one or more of the following determinants:

- cardiac function
- cardiac rhythm
- preload and afterload
- valvular diseases
- heart–lung interactions


Therefore, by examining and comparing the Doppler spectrum, one would be able to deduce some of this information and draw inference about the cardiac function and haemodynamic status ([Fig. 1.2](#)).


This chapter begins by revising ultrasound properties and Doppler physics that are important for the understanding the Doppler spectrum. Important concepts such as Doppler intensity and modal velocity will be discussed. Finally, the principles and applications

of various Doppler modalities, including tissue Doppler, will be presented.

Wave properties revisited

Sound wave

Sound wave is mechanical vibrations of the particles in a medium. The particles only vibrate (oscillate) about an equilibrium (or mean) position, and does not involve permanent displacement of particles ([Video 1.1](#) ). The vibration transfers mechanical energy from one point to another.

In medical ultrasound, the piezoelectric crystals on the surface of transducer act as the sound sources (vibrator). In response to a change in electrical voltage, the piezoelectric crystals vibrate in the MHz range, hence producing ultrasound. Like all sound waves, ultrasound is a longitudinal wave and, as the particles vibrate, alternate regions of high and low pressures, known as *compressions* and *rarefactions*, respectively, are created ([Fig. 1.3A](#)). The distance of the particles from their equilibrium positions against time can be depicted as a sinusoidal wave ([Fig. 1.3](#) and [Video 1.1](#) ).

Sound wave properties

All waves are characterized by three properties:

- **Frequency** (f) is the number of vibrations (cycles) per second and the unit of measurement is Hertz (Hz). Diagnostic ultrasound frequency is typical in the range from 2 to 20 MHz. The reciprocal of frequency ($1/f$) is the *period*, which is the time taken to complete one cycle.
- **Wavelength** (λ) is the length of one complete cycle and is measured in metres.
- **Amplitude** (A) is the magnitude of the wave and is proportional to the number of particles displaced by the vibration ([Fig. 1.3](#)). More energy causes more particles to vibrate. Amplitude is perceived as loudness in sound. In medical ultrasound, it is depicted as brightness (or gain) on the display. The amplitude reduces as ultrasound travels through biological tissues because energy is dissipated in overcoming the viscosity of the tissue, and also through scattering and multiple reflections. This loss of amplitude (energy)

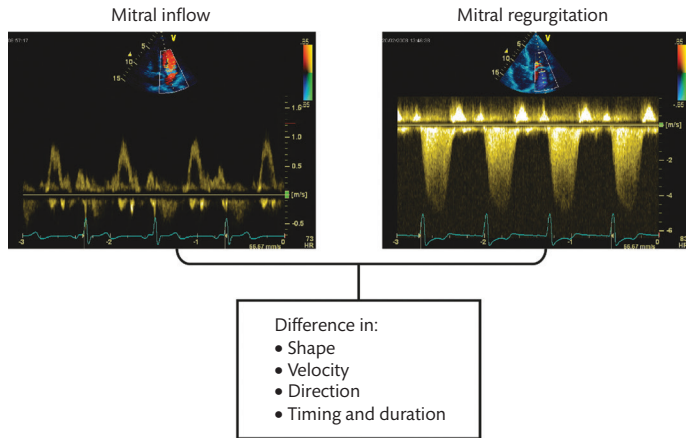


Fig. 1.1 Blood flows are characterized by blood patterns: here are blood flow patterns (also known as Doppler spectra) showing the inflow and regurgitant flows of the mitral valve. Note the differences in shape, velocity, direction of flows (positive and negative), timing, and duration.

with distance travelled is known as *attenuation*, a phenomenon where the amplitude decreases with depth. Sonographers often use the term ‘amplitude’ and ‘intensity’ (I) interchangeably. Although there are differences between the two, we only need to know *intensity* (I) is proportional to the square of amplitude ($I \propto A^2$) and they both refer to the strength of the echo signal in everyday language.

Relationship between frequency, wavelength, and velocity

Velocity (c) is distance the sound wave travels in one second, and is equal to the product of wavelength and frequency:

$$c = \lambda f. \quad \text{Eq.1}$$

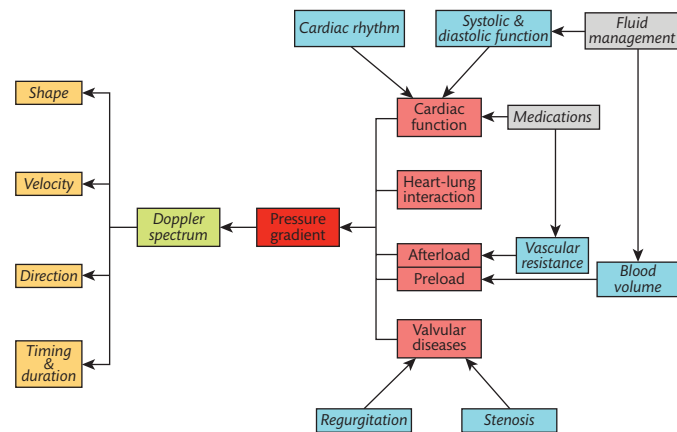


Fig. 1.2 Determinants of Doppler spectrum. Doppler spectrum is governed by the temporal relationships of the pressure gradient between two chambers, which is determined by several major physiological variables including cardiac function, heart–lung interaction, preload and afterload, and valvular diseases. These physiological variables can be altered by other external factors such as medications and fluid administrators.

Ultrasound, regardless of frequency, travels at the same velocity in the same tissue (same tissue density). The velocity changes only when it is travelling in a tissue with different density (e.g. bone vs. muscle), and this is due to the change in wavelength. On the other hand, the frequency remains constant.

Reflection versus penetration

Reflections of ultrasound, commonly known as *echo*, occur where there are changes in tissue *acoustic impedance* (Z), that is, *impedance mismatch* (Table 1.2). As Z is proportional to tissue density (ρ), reflections occur at tissue interfaces (boundaries) where there are differences in ρ .

The percentage of ultrasound reflected ($R\%$) when travelling from tissue 1 to tissue 2 is given by:

$$R\% = \left(\frac{Z_2 - Z_1}{Z_2 + Z_1} \right)^2 \times 100\%, \quad \text{Eq.2}$$

where Z_1 and Z_2 are the acoustic impedances for two adjacent tissues with densities ρ_1 and ρ_2 , respectively. Note that the $R\%$ only depends on the difference of Z s between the two tissues and not on the direction of ultrasound. The percentage of ultrasound left for penetration is $(1 - R\%)$.

Doppler principles

While the frequency of ultrasound is not affected by tissue density, it changes when there is a relative motion between the transducer and the reflector. Since the transducer is mostly stationary when acquiring an image, any change in frequency is assumed to be due to moving reflectors in the body. Common moving reflectors in echocardiography are blood cells, heart valves, and myocardium.

Doppler effect and Doppler shift

When a point sound source vibrates, it emits a series of concentric spherical waves outward. In a two-dimensional plane, this is much like the ripples caused by dropping a stone in a pond (Fig. 1.4). The line joining the particles of the same phase is known as the *wavefront*. The speed of the wavefront travelling away from the sound source is the velocity of the wave, and is constant in that medium.

The frequency of a moving sound source may appear higher or lower, due to the ‘compression’ and ‘spreading out’ of the waveform, depending on the position of the observer (Fig. 1.5). Similarly, a reflector moving towards a stationary sound source compresses the waveform resulting in higher frequency; whereas a reflector moving away from the sound source results in lower frequency due to ‘stretching’ of the wavelength (Fig. 1.6).

Doppler frequency (f_D) or *Doppler shift* (also known as *beat frequency*), refers to the shift in frequency due to the moving red blood cells (RBCs), and is calculated from:

$$f_D = f_e - f_i, \quad \text{Eq.3}$$

where f_D is the Doppler frequency (shift), f_i is the original transmitted frequency, and f_e is the *echo frequency* (Fig. 1.7).

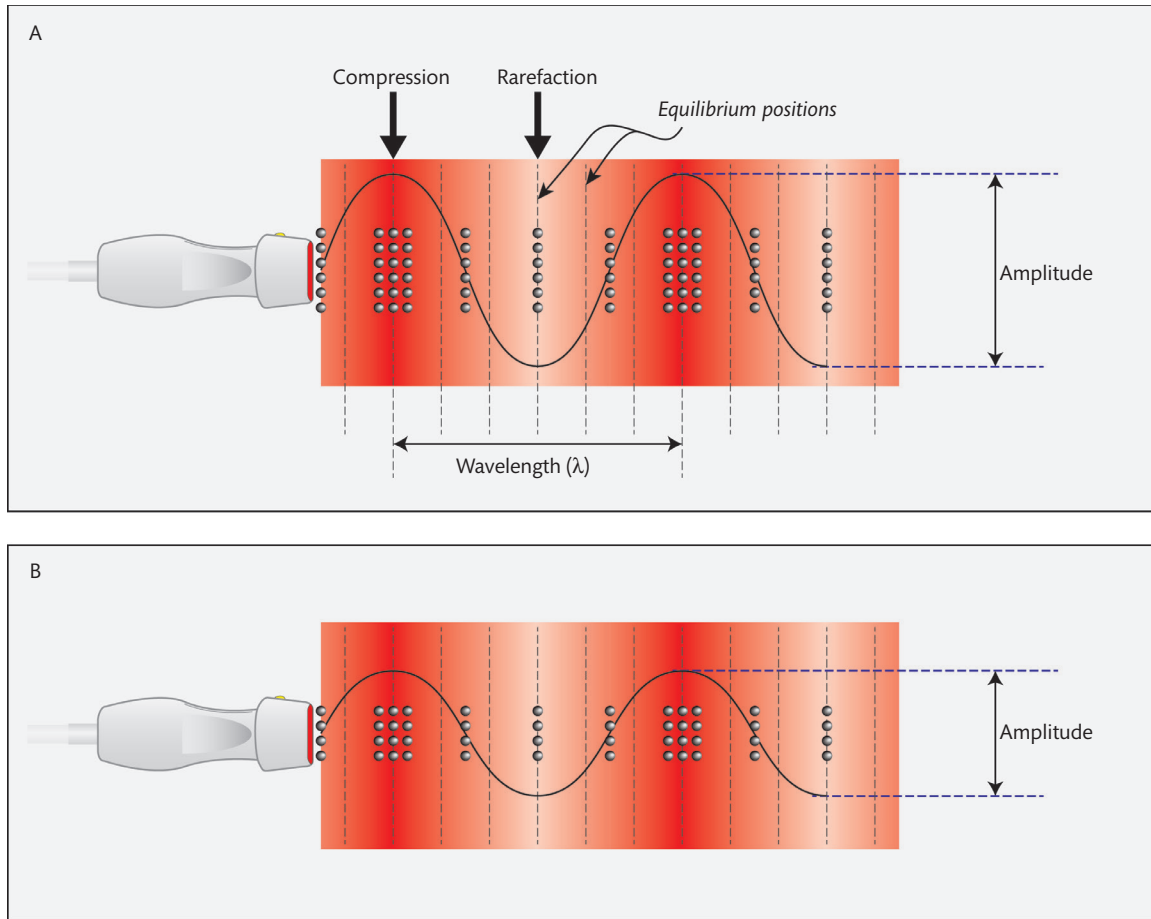


Fig. 1.3 Longitudinal wave. Sound wave is a longitudinal wave where the particles vibrate longitudinally in the direction of wave propagation (refer text for explanation). As the particles vibrate about their equilibrium (mean) positions, they created alternate high and low pressure regions known as compression and rarefactions, respectively. The number of vibrating particles is proportional to the amplitude, and the amplitude determines the intensity (strength) of the ultrasound signal. (A) Large amplitude signal; (B) small amplitude signal.

The Doppler equation

Determination of blood flow velocity is an important element in Doppler echocardiography. Blood flow velocity (v) can be calculated using the Doppler equation:

$$f_D = f_c - f_i = \frac{2 \cdot f_i \cdot v}{c}, \tag{Eq.4}$$

by rearranging:

$$v = \frac{f_D \cdot c}{2 \cdot f_i}, \tag{Eq.5}$$

where c is the *average velocity* of ultrasound in biological tissue and is taken as 1540 m/s (Fig. 1.8A).

The Doppler equation assumes the ultrasound beam is parallel to the blood flow (Fig. 1.10A). If the angle (θ) between the ultrasound beam and the blood flow is greater than zero, the measured velocity (v') will be underestimated by a factor of $\cos\theta$ (Fig. 1.8B). If v is the true flow velocity, then

$$v' = v \cdot \cos\theta, \tag{Eq.6}$$

where θ is known as the *Doppler angle*. Note that v' equals to v when $\theta = 0^\circ$, and v' will be underestimated when θ is greater than 0° .

It is apparent that as θ increases, the error in measuring the velocity also increases (Fig. 1.8C). Ultrasound machines assume θ is zero, hence operators need to minimize θ as much as possible, so that v' approximates v . For practical purpose, θ should be kept less than 20° where the measurement error is less than 10%.

Table 1.1 Velocity of ultrasound in different tissues

Biological tissue or medium	Velocity (m/s)
Muscle	1580
Fat	1459
Kidney	1560
Liver	1550
Blood	1575
Lung	650
Bone	4080
Water	1480
Soft tissue (average)	1540

Table 1.2 Reflection vs. transmission. Examples: typical acoustic impedances

Medium or biological tissue	Z ($\times 10^6$ rayls)
Air	0.0004
Water	1.48
Soft tissue:	
Muscle	1.70
Liver	1.64
Kidney	1.62
Fat	1.38
Blood	1.62
Bone	7.80

The percentage of ultrasound reflected (R%) is the same regardless of the direction of travel. In other words, R% from medium 1 to 2 is the same as from medium 2 to 1. The percentage of transmission can be calculated by $(100\% - R\%)$.

Examples: percentage of reflection at some tissue interfaces

Interfaces	Reflection (%)	Transmission (%)
Air-muscle	99.91	0.09
Fat-muscle	1.08	98.92
Blood-muscle	0.06	99.94
Bone-muscle	90.9	9.1

The power and Doppler spectra

The power spectrum

In laminar flow, RBCs are travelling at a range of velocities in any cross-section of blood vessels at any instance, with the highest

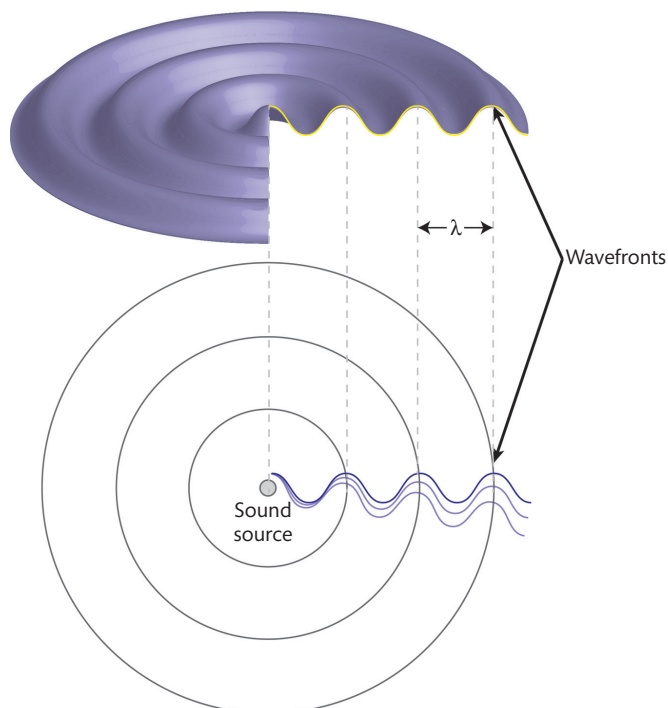


Fig. 1.4 Wave and wavefronts. A schematic diagram showing a two-dimensional representation of wavefronts of a three-dimensional ripple wave (sectioned). A wavefront is the line joining the points where the waves are of the same phase. In this example, the wavefronts represent the contours of the peak of the waves, and the distance between two successive wavefronts represent one wavelength (λ).

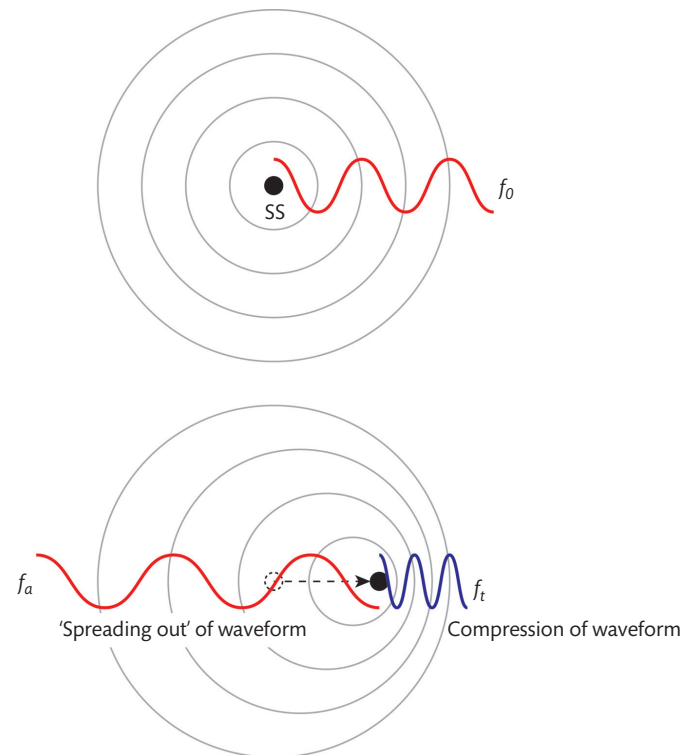


Fig. 1.5 Effects of a moving sound source on wavelengths and frequencies. Upper panel, a stationary sound source (SS) emits sound wave with fixed frequency (f_0) in all directions. Lower panel, the SS moving towards the right compresses the wavefronts on the right side and increases the frequency (f_t). On the other hand, the wavefronts on the left side 'spread out' as SS is moving away resulting in a lower frequency (f_a).

velocities found at the centre of the vessel and lowest at the periphery next to the vessel wall (see next). These different velocities produce a range of echo frequencies (f_e) that combine to give rise to a complex resultant waveform (Fig. 1.9). The ultrasound machine, after receiving the combined complex echo waveform, resolves it into its individual component waveform using a process called *fast Fourier transformation*, or *spectral analysis*. The echo frequencies from each of these individual components are used to calculate the corresponding Doppler frequencies, and converted to individual velocity using the *Doppler equation*. The *distribution of velocities* at any instance can then be plotted in a *power spectrum* (Fig. 1.9). The number of RBC in a Doppler signal determines the amplitude of the wave, which is related to the intensity of the signal (intensity \propto amplitude²) (see earlier) (Fig. 1.10). The intensity is represented by the brightness or *gain* on the display. The *modal velocity*, the velocity at which most of the RBCs are travelling, is the velocity with the highest intensity (gain).

The Doppler spectrum

Blood flow is pulsatile in nature, and the velocities change constantly with time. To examine the changes, blood flow information is collected continuously and the power spectra are also being constructed continuously. A *Doppler spectrum* displaying the relationship between flow velocity (the vertical axis) versus time (the horizontal axis) are constructed by 'stacking' the power spectra obtained at different times (Fig. 1.11). The intensity, which is proportional to the number of RBC, is shown qualitatively as the gain of the signal.

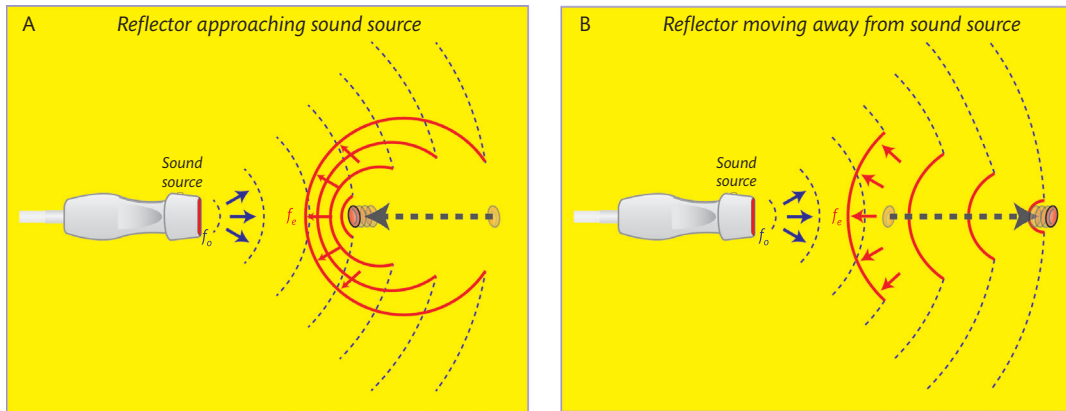


Fig. 1.6 Change in echo frequencies with moving reflectors. A, the transducer emits ultrasound wave of fixed frequency (f_0) (blue wavefronts). Reflector (such as RBC) moving towards the transducer encounters and reflects the wavefronts earlier than a stationary reflector resulting in 'compression' of echo wavefronts (red). Hence, the echo frequency (f_e) appears higher than f_0 . B, when the reflector is moving away from the transducer, it takes longer for the transmitted wavefronts to reach the reflector. As a result, the reflected wave is 'spread out' and f_e is lowered.

Doppler spectra for plug flow and parabolic flow

When blood is first ejected into the aorta, most of the RBCs are travelling at high velocities giving rise to *plug flow*. In plug flow, the bulk of the RBC are moving within a narrow range of high velocities as if all the RBC across the vessel is moving along together as a solid plug (Fig. 1.12). This plug flow profile gradually develops into parabolic flow profile with distance because the layer of blood in touch with the vessel wall is slowed down due to friction at the blood–vessel boundary. This friction (or drag) passes on from the boundary layer inward into the 'core' (see Chapter 3 and Box 3.2). Eventually, the central core flows with the highest velocity, and the velocities decrease towards the boundary (periphery). This is known as *parabolic flow* (Fig. 1.12). As discussed earlier, plug flow is characterized

by narrow spectra whereas parabolic flow gives rise to broad spectra (see Fig. 2.1, Chapter 2, for example of spectral broadening).

Pulsed-wave vs. continuous-wave Doppler

Pulsed-wave Doppler

In pulsed-wave Doppler, the transducer transmits short ultrasound pulses at regular intervals known as *pulse repetition period* (PRP), typically between 80 and 250 μsec . The *pulse duration* (PD) is the 'length' of the pulse and is in the range of 1 to 2 μsec . In other words, for each cycle, the transducer spends less than 2% of the time for transmission. The pulse repetition frequency (PRF), defined as $1/\text{PRP}$, is in the range of 4000 to 12 000 Hz. After transmitting the pulse, the transducer then acts as a receiver until the next pulse is sent. PRP is determined by the *depth of the sample gate*.

To find the blood flow velocities at a particular location, the operator places a *sample gate* (also known as *range gate* or *sample volume*) at that location. Using the depth of the sample gate, the ultrasound machine calculates the *flight time* (t), time taken for the pulse to travel to and back from the sample gate location, by

$$t = \frac{2d}{c}, \quad \text{Eq.7}$$

where d is the depth and c is the average ultrasound velocity in biological tissue. The total distance travelled by the pulse is $2d$. The receiver function of the transducer is then activated briefly to receive the echo at time t after the pulse is transmitted. Since c is 1540 m/s, therefore

$$t = \frac{d}{0.077} \mu\text{sec}. \quad \text{Eq.8}$$

Ideally, the echo should have returned to the transducer before the next pulse is transmitted. In other words, t should be less than PRP. If d is too large, t may exceed the PRP and returns to the transducer *after* the second pulse is transmitted. In this case, the machine may misinterpret that the echo is from the second pulse instead of the one before, and erroneously assuming the echo is from a location much closer than the true location. Therefore, most machines set

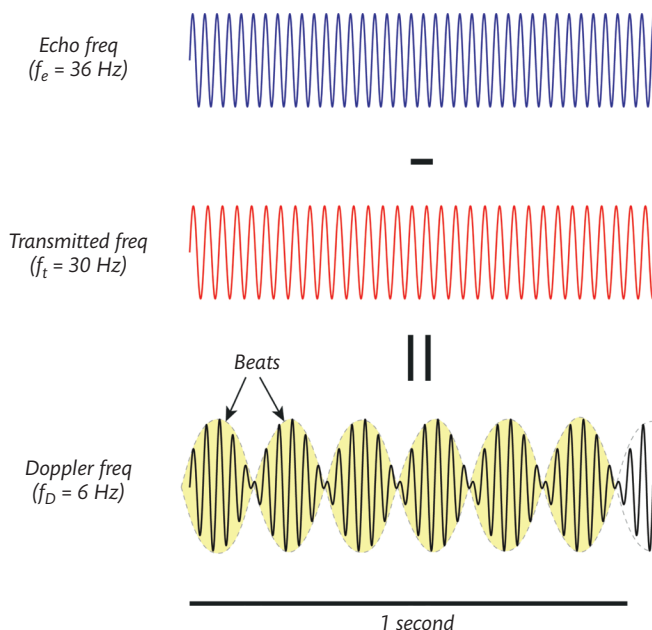


Fig. 1.7 Doppler frequency. The difference between the echo frequency and the transmitted wave frequency ($f_e - f_t$) gives rise to the Doppler frequency (f_D), also known as the beat frequency or Doppler shift. In this example, f_e is 36 Hz and f_0 is 30 Hz. The Doppler frequency, number of beats per second, is therefore $36 - 30 = 6$ Hz.

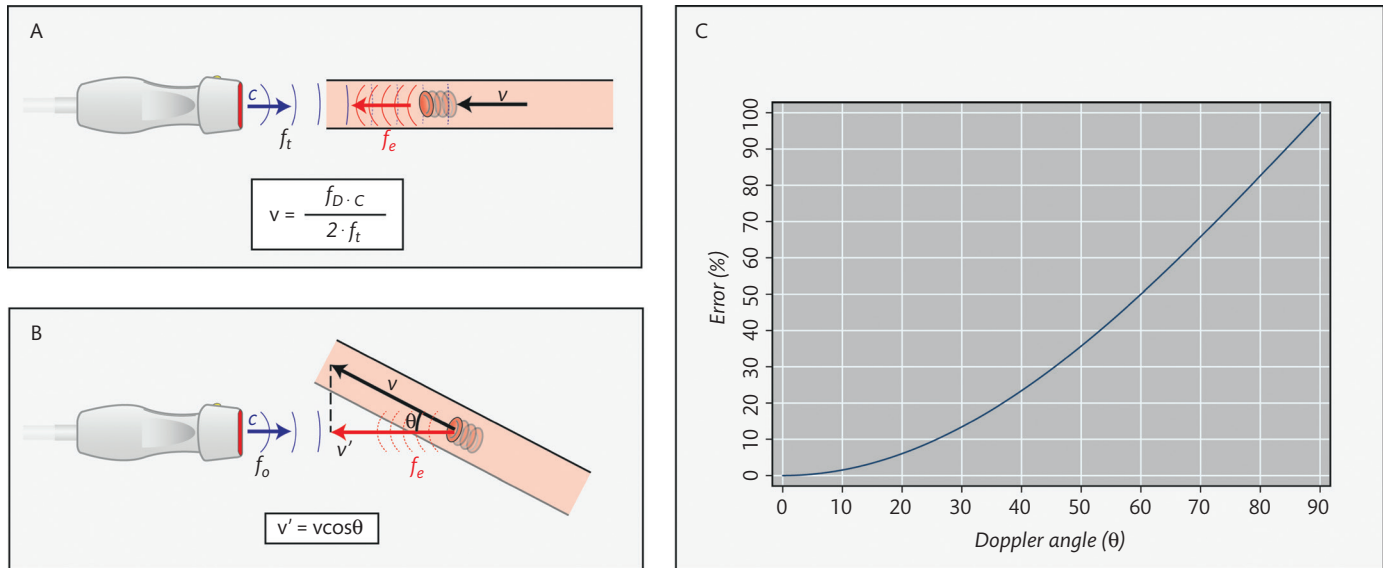


Fig. 1.8 Doppler equation and effects of Doppler angle. (A) The Doppler equation (inset) is valid only when the ultrasound beam is parallel to the blood flow (i.e. Doppler angle $\theta = 0$ degrees). (B) If the Doppler angle θ is greater than zero to the flow, the true blood flow velocity (v) is now underestimated as v' . c is the average speed of ultrasound in biological tissue ($=1540$ m/s); f_t , f_e , and f_D are the transmitted wave, echo, and Doppler frequencies, respectively. (C) The percentage error in estimating blood flow velocity increases curvilinearly with Doppler angle.

a maximum d where t is equal to PRP, and display multiple sample gates if t exceeds PRP.

The size of the sample gate is typically set between 2 and 5 mm but can be adjusted by the operator. A small sample gate size improves *range specificity* (location certainty) and is preferable. However, if

the signal (gain) is weak, then a larger sample gate can be used but this diminishes the range specificity.

The echoes returning from the same location are received and stored for several cycles. Each echo pulse is resolved into individual frequencies by spectral analysis (see previous section and Fig. 1.9).

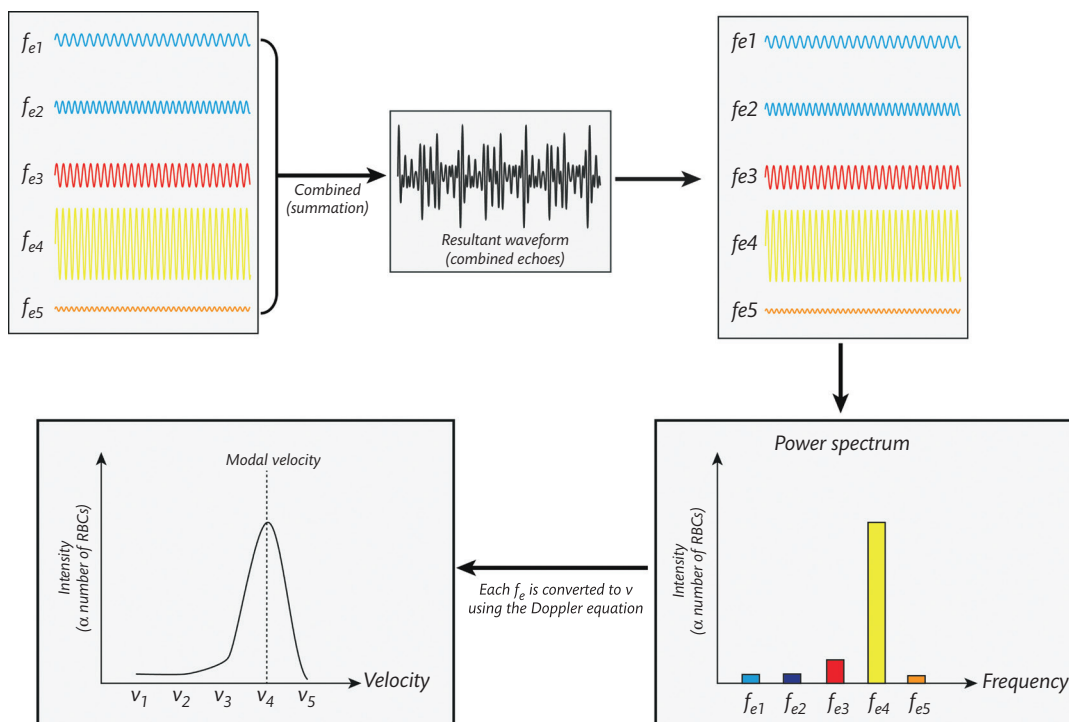


Fig. 1.9 The Doppler power spectrum. At any particular instance, echoes from all RBCs (travelling at different velocities) combine and give rise to complex resultant waveform. This complex waveform is resolved into its individual component frequencies (f_e) using fast Fourier transformation (FFT). A power spectrum showing the distribution of velocities is plotted after converting each frequency to velocity using the Doppler equation. The intensity of each frequency (or velocity) is proportional to the amplitude of the f_e which in turn is decided by the number of RBCs travelling at that corresponding velocity.

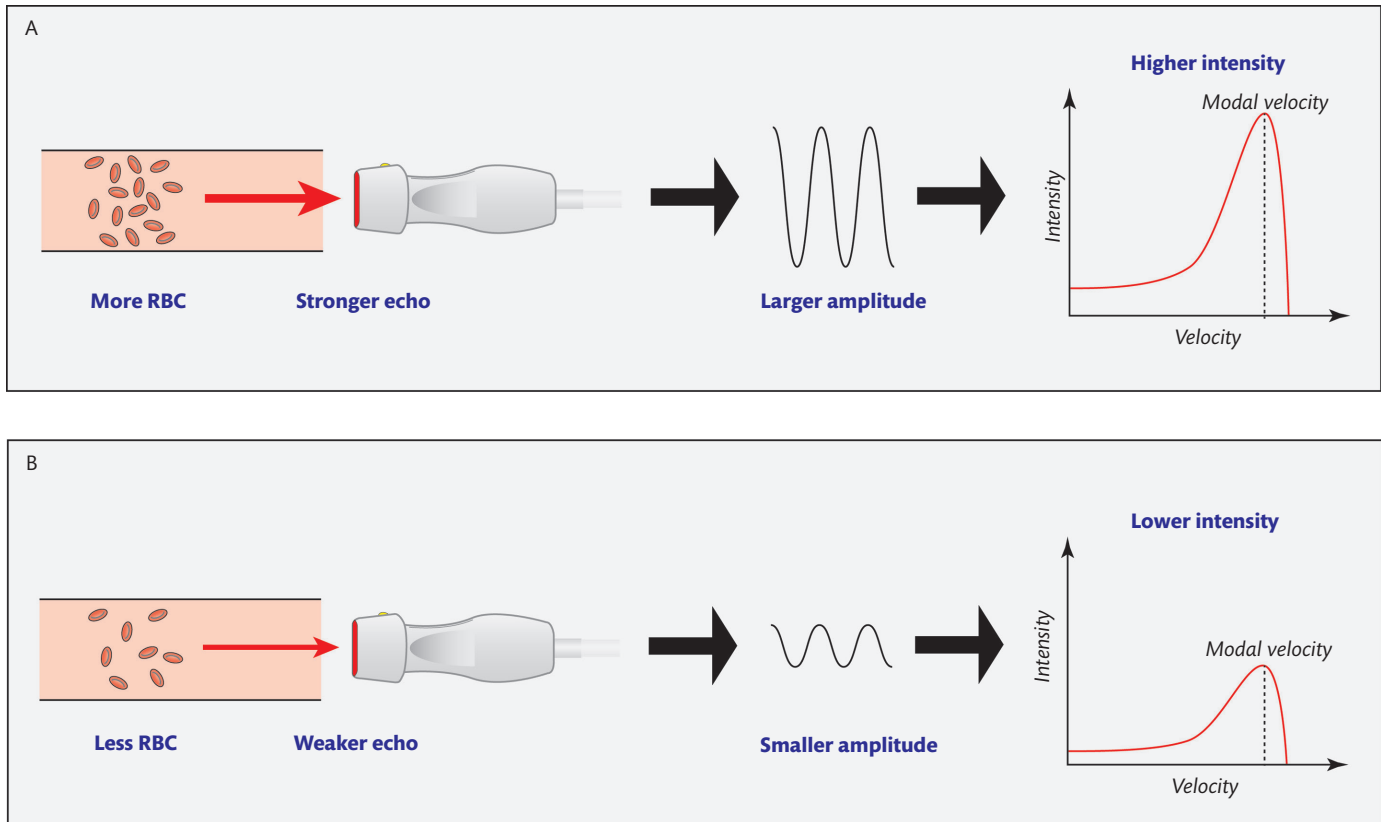


Fig. 1.10 Amplitude and intensity of Doppler signal. The amplitude of the echo is proportional to the number of RBCs. This amplitude is translated into intensity by the ultrasound machine. Modal velocity is the velocity of most of the RBCs.

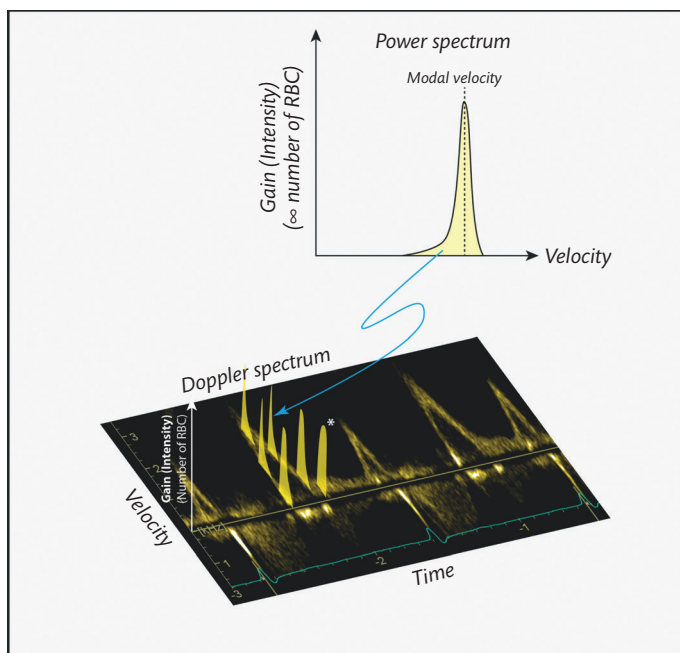


Fig. 1.11 The Doppler spectrum. Doppler spectrum is not to be confused with power spectrum (Fig. 1.12). Doppler spectrum is a plot of velocity against time, and is constructed by combining power spectra from consecutive sampling (times). The y-axis (i.e. intensity) in the power spectrum is displayed as 'gain' (brightness) in the Doppler spectrum, and the x-axis (velocity) becomes the y-axis in the Doppler spectrum. The power spectrum in this example represents one obtained from plug flow, hence resulting in narrow Doppler spectrum. Parabolic flow gives rise to broad spectra (marked with *).

These frequencies are converted to Doppler frequencies and finally to the corresponding velocities using the Doppler equation. Power spectrum is constructed using the velocities and the amplitude information (Fig. 1.13, see also Fig. 1.12). Combining power spectra obtained consecutively gives rise to the Doppler spectrum (Fig. 1.11).

Aliasing in PW Doppler

A minimum of two pulses per beat are required to correctly define the f_D , hence flow velocity. This is achieved by using a high sampling rate (i.e. PRF). In other words, the maximal f_D , hence maximal blood flow velocity (v_{max}), can be detected is:

$$\text{Maximal } f_D = \frac{\text{PRF}}{2}. \quad \text{Eq.9}$$

The aforementioned relationship is known as the *Nyquist limit*, which states that the f_D should not exceed half the sampling frequency (i.e. PRF) or the PRF should be more than twice the f_D .

When the sampling rate is less than two pulses per beat (long PRP), the Doppler frequency, f_D , will be underestimated resulting in a lower velocity (Fig. 1.14). Underestimation of f_D is usually accompanied by a phase shift (ϕ) (Fig. 1.14B). The ultrasound machine interprets this phase shift and displays the aliasing flow in the opposite flow direction resulting in a 'wrap-around' phenomenon (see also Fig. 2.6).

There are four general methods to correct for aliasing:

1. Adjusting the baseline to devote the entire range of velocity range to the correct flow direction. This can double the v_{max} without aliasing.

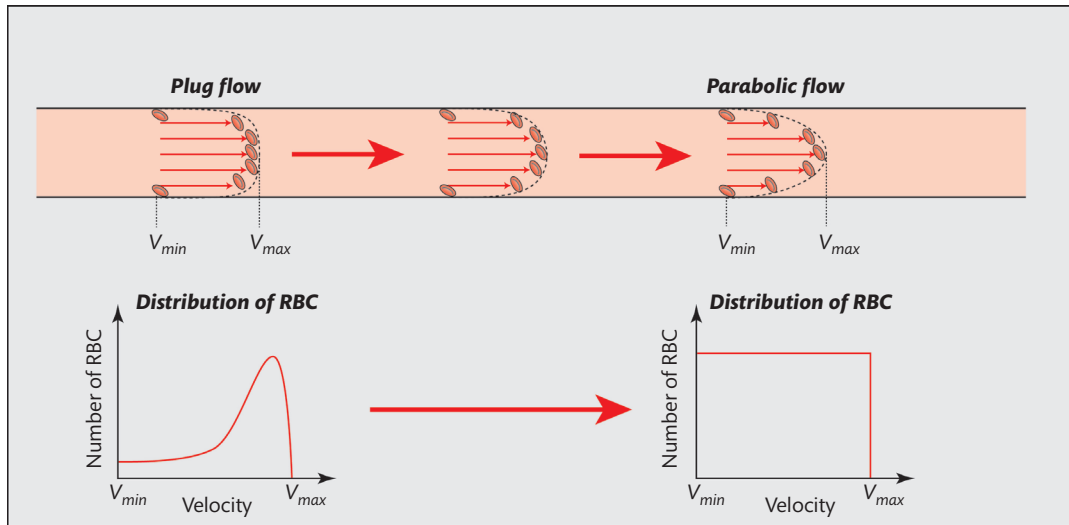


Fig. 1.12 Power spectrum of parabolic flow and plug flow. As blood leaves the left ventricle and travels downstream, the flow profile changes from plug flow to parabolic flow due to viscosity (see Chapter 3). Parabolic flow is characterized by a uniform distribution of velocities, whereas plug flow is characterized by a skewed distribution with most RBCs travelling at higher velocities.

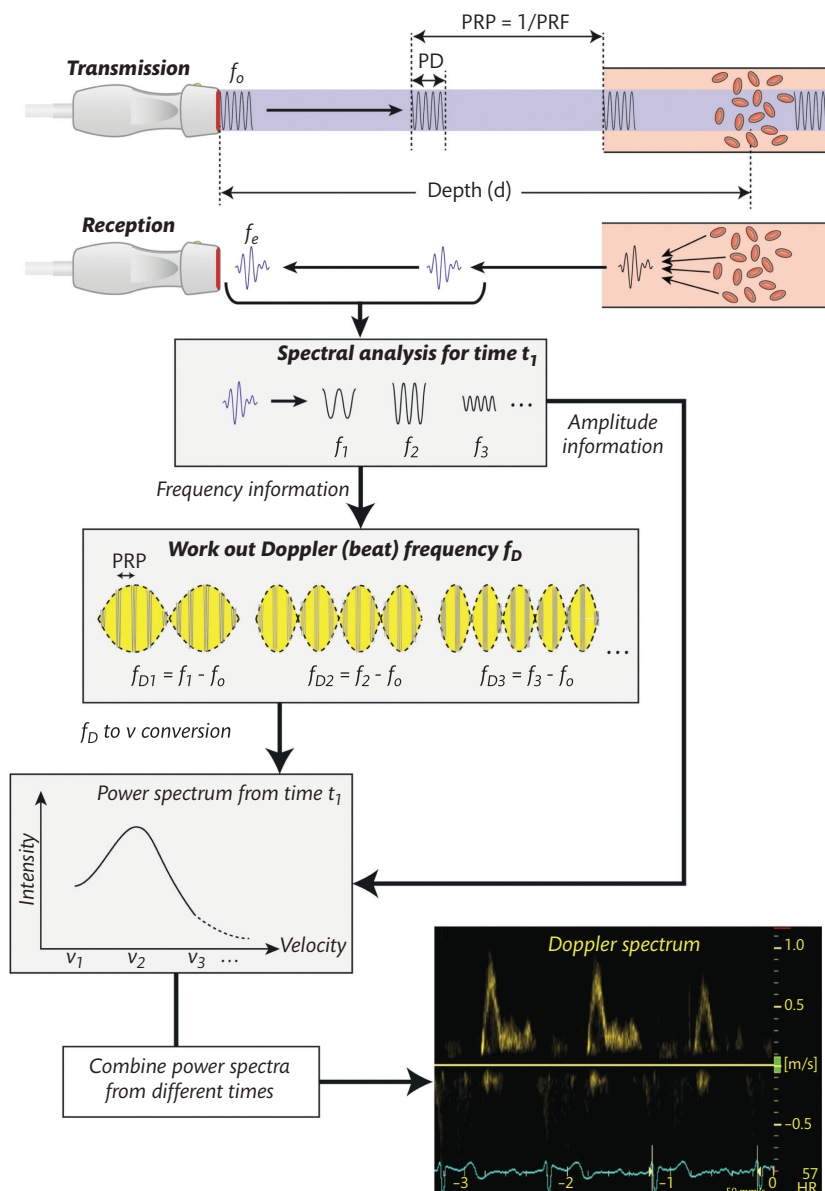


Fig. 1.13 Construction of Doppler spectrum in PW Doppler. Refer to text for explanation; see also Figure 1.15. PRF, pulse repetition frequency; PRP, pulse repetition period; f_n , individual component frequency; f_D , individual Doppler frequency.

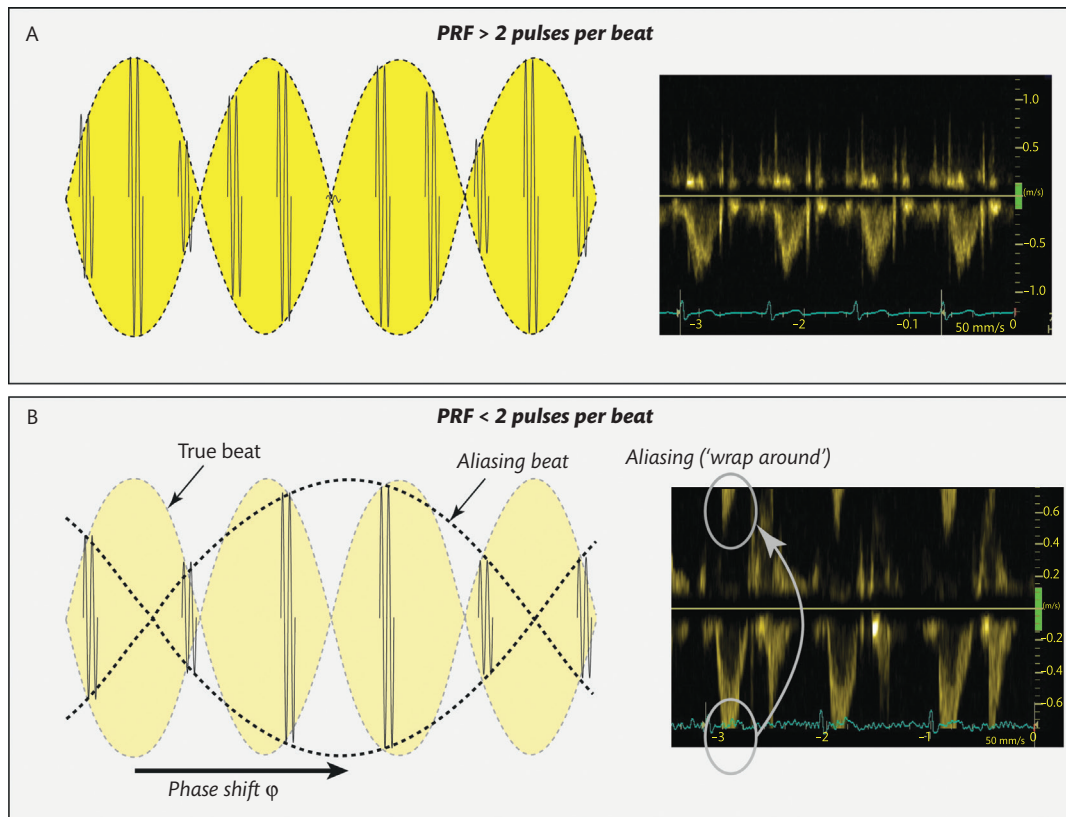


Fig. 1.14 Aliasing. The beat frequency, and hence velocity, can be correctly delineated if the sampling rate, the pulse repetition frequency (PRF), is greater than two per beat (A). The beat frequency will be underestimated if the PRF is less than two per beat resulting in aliasing (B). Phase shift is also present and is responsible for the 'wrap-around'. In (B), instead of depicting the peak velocity as -0.9 cm/s, the peak velocity is presented as $+0.5$ cm/s which is of lower magnitude and opposite sign.

2. Provided that the PRF is not at its maximum, the PRF can be increased by increasing the velocity scale.
3. From Equations (5) and (9),

$$v_{max} = \frac{PRF \cdot c}{4 \cdot f_o} \quad \text{Eq. 10}$$

Hence, reducing the transducer frequency (f_o) increases v_{max} (Box 1.1).

4. PRF is inversely proportional to the depth (d) of the sample volume:

$$PRF = \frac{c}{2d} \quad \text{Eq. 11}$$

Reducing the depth can therefore increase the PRF (Box 1.1). Unfortunately, reducing depth in the same acoustic window is often not possible as the PW Doppler measurements are location specific. However, using other acoustic windows may help in reducing the depth (e.g. parasternal rather than apical windows).

Some machines offer a 'high PRF' option. However, a depth that is beyond what the PRP can cover results in two or more sampling volumes, hence two or more signals being interrogated. Positioning

the extra sample gate at a location where no flow is present removes the ambiguity. Otherwise, continuous-wave Doppler should be deployed (Fig. 2.6).

Continuous-wave Doppler

Continuous-wave (CW) Doppler splits the piezoelectric crystals on the transducer into two sets for data acquisition: (1) one set (usually 50%) of the crystals are used for ultrasound transmission; and (2) the other set for receiving echoes. Ultrasound transmission and reception are simultaneous and continuous in CW Doppler. The beat frequency is worked out as previously described (see *Doppler principles* and Fig. 1.7).

Range ambiguity

As CW Doppler receives echo signal continuously, one major problem is that all flow signals along the beam path will be received and interrogated giving rise to the issue of *range ambiguity*—the inability to resolve the specific location of flow signal when two or more flows are present, or the uncertainties in the actual location from which the Doppler signals occur. This gives rise to a *masking* effect, where a high velocity signal masks the low velocity signal. For example, if a low flow signal lies in the same beam path as a high flow signal, such as left ventricular outflow tract (LVOT) and stenotic aortic valve, the two signals overlap with the high velocity stenotic flow, thus masking the low velocity LVOT flow (Fig. 1.15). Masking is usually not an issue if only the highest velocity is the focus of the study because signals are not additive.

Box 1.1 Maximal velocity in PW Doppler

Calculate the maximal velocity that can be measured if the PRF is 12 000 Hz and the frequency of the transducer (f_o) is 3 MHz (assuming $c = 1540$ m/s).

The maximal velocity (v_{max}) is given by:

$$v_{max} = \frac{PRF \cdot c}{4 \cdot f_o}$$

by substitution:

$$v_{max} = \frac{12000 \cdot 1540}{4 \cdot 3 \times 10^6} \text{ms}^{-1} \approx 1.5 \text{ms}^{-1}$$

Calculate the maximal velocity that can be measured if the depth (d) is 10 cm (0.1 m) and the frequency of the transducer (f_o) is 3.5 MHz (assuming $c = 1540$ m/s).

The PRP is given by $PRP = \frac{2 \cdot d}{c}$, therefore $PRF = \frac{c}{2 \cdot d}$.

Substituting PRF in the first equation:

$$v_{max} = \frac{PRF \cdot c}{4 \cdot f_o} = \frac{c^2}{8 \cdot d \cdot f_o}$$

$$v_{max} = \frac{1540^2}{8 \cdot 0.1 \cdot 3.5 \times 10^6} \approx 0.85 \text{ms}^{-1}$$

What if the frequency of the transducer (f_o) is reduced to 2 MHz?

$$v_{max} = \frac{1540^2}{8 \cdot 0.1 \cdot 2 \times 10^6} \approx 1.48 \text{ms}^{-1}$$

Aliasing in CW Doppler

Aliasing is not observed in CW Doppler because Doppler pulses are not used and therefore the issue of the Nyquist limit does not exist.

Applications of PW and CW Doppler

PW and CW Doppler complement each other in echocardiography applications:

- **PW Doppler:** The main advantage of PW Doppler is that the operator can choose the location where the velocity is to be measured—only the echoes returning to that location are being interrogated. However, PW Doppler cannot be used to measure high velocity flow because there is a limit on v_{max} imposed by PRF.
- **CW Doppler:** This is ideal for measuring high velocity flows, such as regurgitations, stenoses, and shunts. The inability to resolve the location of flow signals is the main disadvantage of CW Doppler. However, this is usually not a concern as the flow with the highest velocity masks other flows with lower velocities.

Colour-flow Doppler (CFD)

Colour-flow Doppler provides real-time visualization of blood flow on the display. A detailed description of CFD instrumentation is beyond the scope of this book. Briefly, when CFD function is activated, the ultrasound machine places a 'CFD window' (or CFD box) with multiple PW Doppler gates over the 2D images. The echoes from these gates are interrogated using PW Doppler and the *mean velocities* of blood flow from each of these gates are displayed on the screen using a colour that matches the colour-flow map (Fig. 1.16) [2,3]. As a result, blood flow information is displayed along with the 2D

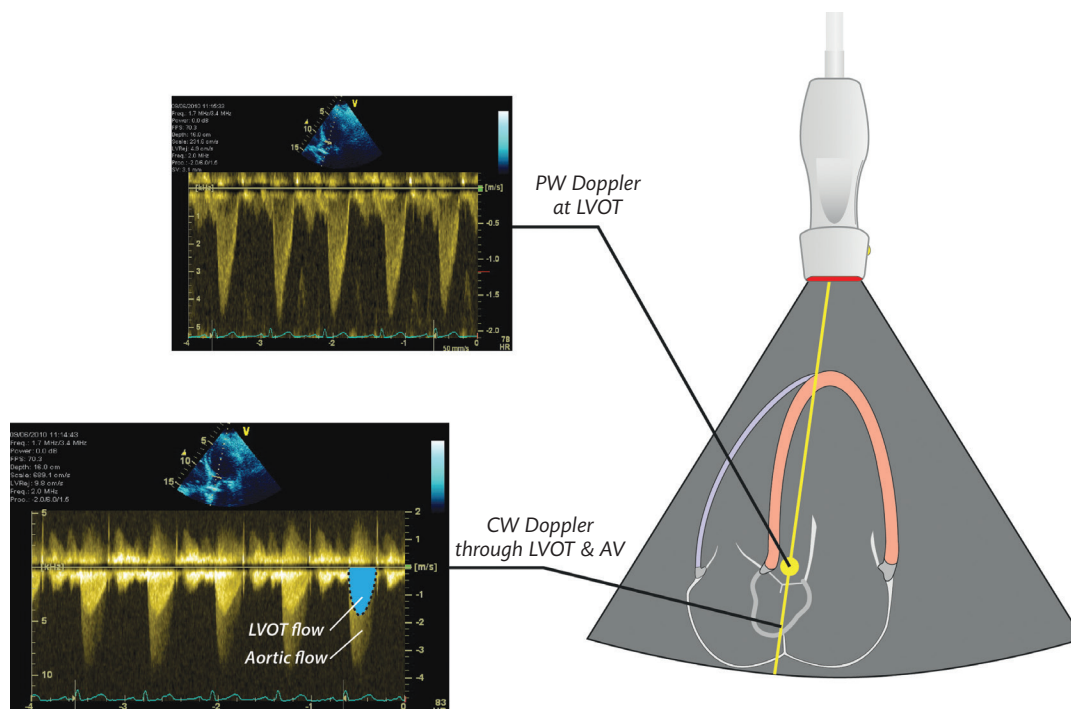


Fig. 1.15 Range ambiguity and 'masking' in CW Doppler. CW Doppler cannot resolve the location of flow signal. All signals along the cursor will be picked up and interrogated resulting in masking of low velocity signals by high velocity signals.

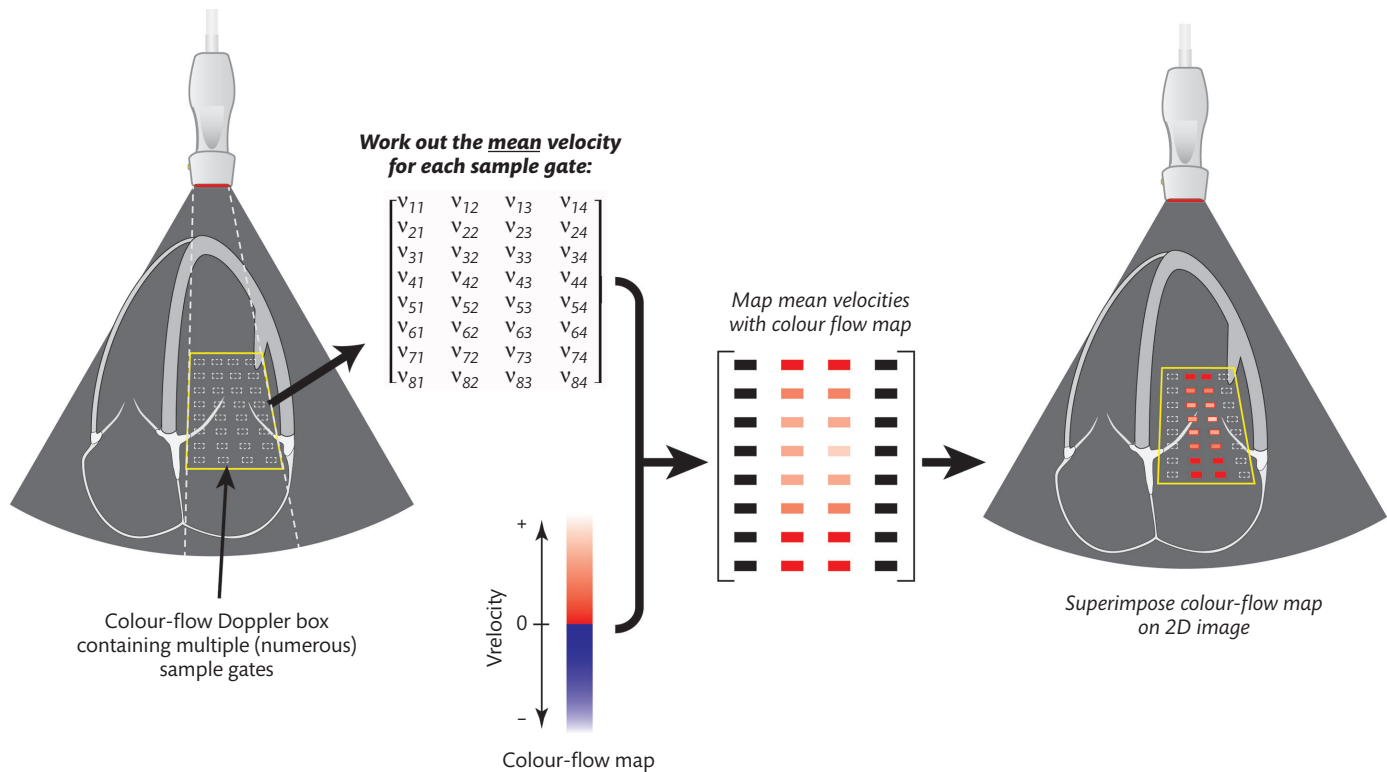


Fig. 1.16 Colour-flow Doppler. A colour-flow Doppler box contains numerous PW sample gates. The echoes of these sample gates are interrogated and the mean velocity for each sample gate calculated. The mean velocities are represented by the corresponding colours in a colour-flow map. The colour-flow is superimposed on a 2D image. v_{rc} , the mean velocity for the sample gate in row r and column c .

image so that the direction, the mean velocity, and location of the flow can be appreciated.

Direction of blood flow

The direction of blood flow, with reference to the transducer position, is represented by different *hue* (colour) in CFD. By convention, blood flow direction is displayed as 'Blue Away, Red Towards' the transducer (BART) (Fig. 1.17A). As the mean velocities are determined by the Doppler principle, the detection of the velocities will be subjected to the same Doppler angle limitation. Therefore, flows perpendicular (90°) to the transducer do not register any hue and appear black (Fig. 1.17B). However, some flows can still be registered at the two ends (away from the midline) by phased-array or curvilinear transducers because the beam directions are at an angle (less than 90°) with the flow (Fig. 1.17B).

Area of colour

The area of a particular colour represents the number of sample gates with the same mean velocity. Hence, a larger area of the same colour implies a larger amount of blood flowing at that same mean velocity (Fig. 1.16). Of note, the area does not reflect flow velocity; only the colour correlates with velocity (see next).

Velocity of blood flow

In CFD, the intensity of the colour denotes blood flow velocity (*cf.* the intensity denotes number of RBC in CW and PW Doppler). Dark or deep shades usually represent low velocities whereas light shades

represent high velocities (Fig. 1.18A). As motion of the myocardium can also be detected by CFD, a *wall filter* is also applied to eliminate the low range myocardial velocities.

In parabolic or plug flow, the range of mean velocities is relatively narrow (and hence small *variance*), and the maximal mean velocity is usually within the Nyquist limit (or v_{max}) (Fig. 1.18A). However, in situations where turbulence is present or flow velocity is high, as in regurgitations and stenosis, the range of mean velocities is large (and hence large variance) and exceeds the Nyquist limit (Fig. 1.18B). As in PW Doppler, velocities that exceed the Nyquist limit appear as *aliasing* and 'wrap-around' the colour-flow map. When the latter occurs, the aliasing velocities will be depicted in the traditional 2-colour *colour Doppler map* as the opposite flow colour (blue or red), or as different colours such as green or yellow if *variance Doppler map* is used (Fig. 1.18B and Fig. 1.19). The boundary between two hues represents blood flowing at the aliasing velocity (v_{max})—the *isovelocity contour* in colour-flow 2D images (Fig. 1.20). In the three-dimensional perspective, the boundary forms an *isovelocity shell* (or surface area) and is used for calculation of effective regurgitant or stenotic orifice (Box 1.2). Shifting the baseline has the effect of increasing or decreasing the aliasing velocity, thereby moving the *isovelocity shell* towards or away from the transducer (Fig. 1.20).

Increasing the scale of the colour-flow map increases the PRF, hence v_{max} . In some machines, this also increases the wall filter, hence filtering out the slow-motion artefacts from myocardial and valve motions.